Biogeosciences

Research article

Particle fluxes by subtropical pelagic communities under ocean alkalinity enhancement

Philipp Suessle[1], Jan Taucher[1], Silvan Urs Goldenberg[1], Moritz Baumann[1], Kristian Spilling[2,3],
Andrea Noche-Ferreira[3,4], Mari Vanharanta[2,5], and Ulf Riebesell[1]

[1]GEOMAR Helmholtz Centre for Ocean Research Kiel, Wischhofstraße 1–3, 24148 Kiel, Germany
[2]Marine and Freshwater Solutions, Finnish Environment Institute, Helsinki, Finland
[3]Centre for Coastal Research, University of Agder, Kristiansand, Norway
[4]Department of Natural Sciences, University of Agder, Kristiansand, Norway
[5]Tvärminne Zoological Station, University of Helsinki, Hanko, Finland

Correspondence: Philipp Suessle (philippsuessle@gmx.de)

Abstract. Ocean alkalinity enhancement (OAE) has been proposed as a carbon dioxide removal technology (CDR), allowing for long-term storage of carbon dioxide in the ocean. By changing the carbonate speciation in seawater, OAE may potentially alter marine ecosystems with implications for the biological carbon pump. Using mesocosms in the subtropical North Atlantic, we provide first empirical insights into impacts of carbonate-based OAE on the vertical flux and attenuation of sinking particles in an oligotrophic plankton community. We enhanced total alkalinity (TA) in increments of $300\,\mu\mathrm{mol}\,\mathrm{kg}^{-1}$, reaching up to $\Delta\mathrm{TA} = 2400\,\mu\mathrm{mol}\,\mathrm{kg}^{-1}$ compared to ambient TA. We applied a $p\mathrm{CO}_2$-equilibrated OAE approach; i.e., dissolved inorganic carbon (DIC) was raised simultaneously with TA to maintain seawater $p\mathrm{CO}_2$ in equilibrium with the atmosphere, thereby keeping perturbations of seawater carbonate chemistry moderate. The vertical flux of major elements, including carbon, nitrogen, phosphorus, and silicon, as well as their stoichiometric ratios (e.g., carbon-to-nitrogen ratios), remained unaffected over 29 d of OAE. The particle properties controlling the flux attenuation, including sinking velocities and remineralization rates, also remained unaffected by OAE. However, we observed abiotic mineral precipitation at high OAE levels ($\Delta\mathrm{TA} = 1800\,\mu\mathrm{mol}\,\mathrm{kg}^{-1}$ and higher) that resulted in a substantial increase in particulate inorganic carbon (PIC) formation. The associated consumption of alkalinity reduces the efficiency of CO_2 removal and emphasizes the importance of maintaining OAE within a carefully defined operating range. Our findings suggest that carbon export by oligotrophic plankton communities is insensitive to OAE perturbations using a CO_2 pre-equilibrated approach. The integrity of ecosystem services is a prerequisite for large-scale application and should be further tested across a variety of nutrient regimes and for less idealized OAE approaches.

1 Introduction

Carbon dioxide removal (CDR) on a grand scale is likely to be needed to restrict global warming to between 1.5 and 2 °C (Masson-Delmotte et al., 2021). Oceans play a key role in buffering the climate by absorbing heat and CO_2, and ocean-based CDR could further enlarge the oceanic carbon pool (GESAMP, 2019). Ocean alkalinity enhancement (OAE) has been proposed as one such measure (National Acadmies of Sciences, 2021). Simulating natural rock weathering, it elevates the oceans' total alkalinity (TA) by dissolving large amounts of minerals in seawater (Kheshgi, 1995; González and Ilyina, 2016). The associated change in carbonate speciation increases the capacity of seawater to take up CO_2 (Köhler et al., 2010; Hartmann et al., 2013). OAE has several potential benefits compared to other CDR technologies (Taylor et al., 2016). It does not compete for freshwater, land, or nutrient use (Smith et al., 2016); can rely on existing infrastructure from the mining industry (Renforth and Henderson, 2017); is applicable to large regions of the open

ocean (Köhler et al., 2010); and additionally counters effects of ocean acidification (Doney et al., 2009; Gattuso et al., 2015). Different modeling studies suggest a potential CO_2 uptake by OAE ranging from 14–41 $Gt CO_2 yr^{-1}$ (Paquay and Zeebe, 2013; González and Ilyina, 2016; Feng et al., 2017). For comparison, natural rock weathering currently locks up 1.1 $Gt CO_2 yr^{-1}$ (Ciais et al., 2014).

Before large-scale deployment, the safety of OAE for marine organisms and ecosystem services has to be assured. OAE-related changes in pH, ion concentrations, and the carbonate saturation state (Ω) would be permanent and may be elevated to well above current and pre-industrial levels (Feng et al., 2017; Renforth and Henderson, 2017). Such shifts in carbonate speciation might influence marine organisms (Bach et al., 2019a), analogous to effects observed for ocean acidification. In turn, calcifying organisms may theoretically benefit from, for example, lime-based alkalinity enhancement, as the enhanced $CaCO_3$ saturation state (through excess of Ca^{2+} and CO_3^{2-} ions) and increased pH may facilitate $CaCO_3$ precipitation, allowing calcifiers to allocate more energy towards growth or other metabolic processes (Jokiel, 2011; Monteiro et al., 2016; Bach, 2015). Riebesell et al. (2017) demonstrated that varying pH levels on natural communities caused large differences in population sizes of the prominent calcifying phytoplankton species *Emiliania huxleyi*. If there are ecological impacts of OAE, these would likely propagate through communities altering ecosystem services such as the biological carbon pump, which sequesters CO_2 into the deep ocean for hundreds to thousands of years (Boyd et al., 1999).

Several studies have revealed the influence of abiotic conditions on the magnitude and efficiency with which particulate organic carbon (POC) from photosynthetic biomass production is exported by gravitational settling (Schmittner et al., 2008; Taucher and Oschlies, 2011; Bopp et al., 2013; Martínez-García et al., 2014). Assuming a proliferation of calcifiers, organic carbon export could increase in response to higher carbonate ballasting (Honjo et al., 2008). Carbonate ballast is generally described by the fraction of particulate inorganic carbon (PIC) to particulate organic carbon (POC) (Klaas and Archer, 2002).The mineral's excess density (Francois et al., 2002) would increase sinking velocities (SVs) of the export flux (Bach et al., 2016). With more carbonate ballasting, particles would on average sink deeper, thus storing atmospheric CO_2 for longer (Kwon et al., 2009). Additionally, particles containing $CaCO_3$ have shown reduced carbon remineralization rates (C_{remin}), possibly due to protection of POC in mineral shells, further increasing carbon transport to depth (Engel et al., 2009). A proliferation of calcifiers, however, could also hamper OAE's capability to store atmospheric carbon (Bach et al., 2019a). The CO_2 release associated with calcification is known as the carbonate counter pump and reflects a positive feedback on atmospheric carbon levels (Koeve, 2002; Salter et al., 2014). Recent laboratory-based OAE experiments (Moras et al., 2022;

Hartmann et al., 2023) demonstrated an alkalinity consumption due to abiotic PIC precipitation, further highlighting its importance for larger-scale OAE applications and implications on carbon export.

The CO_2 sequestration potential of the biological pump also hinges on the stoichiometric ratios of carbon to other macronutrients within the export flux (Shaffer, 1996; Schneider et al., 2003; Passow and Carlson, 2012). An OAE-induced community restructuring could change the nitrogen need per unit of exported carbon, binding the potential magnitude of carbon export to the supply of the limiting nutrient (Hessen et al., 2004). Such a change in ratios of carbon to particulate organic nitrogen (POC : PON) has also been noted in response to changing heterotrophic processes under ocean acidification (Taucher et al., 2021), implying that similar effects might occur under OAE, and further highlights the importance of stoichiometric ratios for carbon sequestration. Whether or not OAE induces substantial changes in species communities and their mediation of the oceans' natural carbon sequestration via the biological pump remains to be seen.

Theoretically, OAE is conceivable in two different approaches. While one merely enhances alkalinity, letting CO_2 equilibrate with the atmosphere post-application, the other approach entails adding solutions where CO_2 is already at equilibrium with the atmosphere, resulting in milder carbonate chemistry perturbations (so-called pre-equilibrated approach). Here, we examined influences of CO_2 pre-equilibrated, carbonate-based ocean alkalinity enhancement on drivers of the biological carbon pump. Using mesocosms in the subtropical North Atlantic, we examined whether OAE (with a doubling of the natural seawaters alkalinity) changes the magnitude and the stoichiometry of the carbon export flux and alters particle properties. If so, to what extent does alkalinity consumption or enhanced ballasting through calcification occur. With this first study on carbon export properties in a natural plankton assemblage, we provide urgently needed understanding of the biogeochemical effects of OAE.

2 Material and methods

2.1 Experimental setup

On 8 September 2021, nine in situ mesocosms were deployed in the harbor of Taliarte (27°59′24″ N, 15°22′8″ W; east coast of Gran Canaria, Spain). Each mesocosm was comprised of a 2.5 m long transparent cylindrical polyurethane foil (Ø = 2 m) with a 1.5 m long conical sediment trap attached below. A polyethylene frame kept the mesocosm bags afloat, and between sampling, mooring and pulley systems allowed moving the construction 2 m away from the pier, thereby reducing its influence on the light regime. The mesocosms were filled with seawater from ~ 100 m outside the harbor (water depth at collection site ~ 20 m). Using a peristaltic pump, water from 2–10 m depth (within the surface

mixed layer; Barton et al. 1998, but avoiding benthic impact) was filtered (< 3 mm) and gathered in an intermediate storage volume, from where each mesocosm simultaneously received ~ 8 m^3 in total. In order to reduce stress on the organisms, the speed of the peristaltic pump averaged ~ 17.35 L min^{-1}, and the entire process lasted ~ 7 h (for further technical details, see Bach et al., 2019b). Filling was done on 10 September and marks Day 0 of the experiment. CTD casts (CTD60M, Sea & Sun Technology GmbH, Trappenkamp, Germany) for temperature, salinity, pH, turbidity, oxygen (O$_2$), and photosynthetically active radiation prior to treatment addition assured that the environmental conditions of water pumped into the mesocosms were as close as possible to those expected for the surface mixed layer of the given oceanographic setting and season (Barton et al., 1998). OAE was simulated in a pCO$_2$-equilibrated OAE approach, meaning that dissolved inorganic carbon (DIC) was raised simultaneously with TA to maintain seawater pCO$_2$ in equilibrium with the atmosphere, thereby keeping perturbations of seawater carbonate chemistry (e.g., pH, Ω_{Ar}) as low as possible. This contrasts non-equilibrated OAE, in which only TA would be increased (while DIC remains constant), leading to much larger transient changes in carbonate chemistry until seawater pCO$_2$ reaches equilibrium with the atmosphere due to air–sea gas exchange. Accordingly, a pre-equilibration of OAE solutions with CO$_2$ represents the least impactful, most optimistic OAE scenario. The OAE treatment in our mesocosm experiment was realized by adding CO$_2$-equilibrated solutions of sodium carbonate and sodium bicarbonate (NaHCO$_3$/Na$_2$CO$_3$ in deionized water) on Day 4. With a custom-built device (see Riebesell et al., 2013, for technical details), each 22 L solution was spread evenly across the water column within 2.5 min. While one mesocosm was only treated with deionized water (control), the remaining eight received increments of ΔTA $= 300$ µmol kg^{-1}, resulting in 4689.3 µmol kg^{-1} (Day 7) for the highest treatment level. This equaled double the alkalinity of the natural seawater. For details on changes in carbonate chemistry parameters, see Table S1. The mooring of the mesocosms was randomized along the pier of the harbor, and the experimental setup enabled us to monitor pelagic communities and biogeochemical responses to OAE for 29 d.

2.2 Sampling procedure and maintenance

In general, sampling was done every 2 d between 09:00 and 12:00 UTC. Additionally, to follow any biological responses related to the filling process, daily sampling was conducted prior to the alkalinity addition. Bulk water samples were taken with a polypropylene pipe, integrating the upper 2.3 m of the water column. On each sampling occasion, 40–60 L (8–12 tubes) of water was sampled per mesocosm. The water was stored in the dark and at in situ temperature in several carboys and transported back to the lab facilities for analysis of chlorophyll a (Chl a), TA and

dissolved inorganic carbon (DIC), dissolved inorganic nutrients (NO$_3^-$ + NO$_2^-$, PO$_4^{3-}$, Si(OH)$_4$), and water column particulate matter (PM$_{\mathrm{WC}}$). Other measurements conducted during the study included analysis of primary productivity, photosynthetic pigment analysis, phyto- and microzooplankton analysis, and prokaryotic heterotrophic production. A CTD60M (Sea & Sun Technology GmbH, Trappenkamp, Germany) was cast for additional abiotic parameters such as temperature, salinity, pH, turbidity, oxygen (O$_2$), and photosynthetically active radiation. Particulate matter from the sediment trap (PM$_{\mathrm{ST}}$) was collected using a manual vacuum pump, not exceeding 0.3 bar during the pumping. Stored in 5 L glass bottles (Schott Scandinavia A/S, Kgs. Lyngby, Denmark), the sediment was kept in the dark until further processing in the lab (see Boxhammer et al., 2016, for technical details). Homogenous subsamples were taken after resuspension of the sediment by gentle rotation of the glass bottles. The subsamples were used for determination of carbon-specific remineralization rates (C$_{\mathrm{remin}}$) and particle SVs as described below.

The inside of the mesocosm walls was cleaned every 4 to 6 d with brushes to prevent nutrient consumption and shading from organisms growing on the walls (for a detailed experimental schedule, see Paul et al., 2024). To further counteract shading, cleaning from the outside was done three times during the experiment by divers equipped with brushes. During cleaning on Day 16, the sediment hose of mesocosm ΔTA$_{900}$ detached. Pumping PM$_{\mathrm{ST}}$ on the subsequent sampling day was not possible; thus SV measurements on Day 17 are missing for this mesocosm. Measurements of SVs and C$_{\mathrm{remin}}$ on Day 19 however are not discarded, as they did not significantly differ from other treatment levels on that day. Yet interpretation should be done with care, as the period for PM$_{\mathrm{ST}}$ settlement was ~ 5 h less than usual.

2.3 Drivers of the biological carbon pump

2.3.1 Export fluxes and stoichiometry

PM$_{\mathrm{ST}}$ material was prepared for analysis of total particulate carbon and nitrogen (TPC/N$_{\mathrm{ST}}$), particulate organic carbon, nitrogen and phosphorus (POC/N/P$_{\mathrm{ST}}$), and biogenic silica (BSi$_{\mathrm{ST}}$) after subsampling. First of all, particles were separated from the seawater. To increase flocculation and coagulation, 3 mol L^{-1} of ferric chloride (FeCl$_3$) was added to the 5 L bottles with sediment material, followed by the addition of 3 mol L^{-1} NaOH to counteract the decreasing pH, promoting an effective particle collection process as shown by previous research (Boxhammer et al., 2016). After 1 h of settlement, the supernatant was decanted, and the remaining flocculated material was centrifuged for 10 min at 5.200 g in a 6–16KS centrifuge (Sigma Laborzentrifugen GmbH, Osterode am Harz, Germany). A second centrifugation step for 10 min at 5.000 g in a 3K12 centrifuge (Sigma) yielded solid sediment pellets. The pellets were stored at -20 °C

Table 1. Experimental design displaying the increments of TA increase relative to the natural background alkalinity of 2402.7 µmol kg^{-1}.

OAE (ΔTA µmol kg^{-1})	0	300	600	900	1200	1500	1800	2100	2400
Symbol	▲	●	■	◆	▼	●	■	◆	▲

and transported back to Kiel for further processing. At GEO-MAR, samples were freeze-dried to remove remaining moisture and ground to a fine homogenous powder in a cell mill (Edmund Bühler GmbH, Bodelshausen, Germany). The sediment powder was stored in a dark and cool place in glass or plastic vials until further processing. Sediment powder was transferred to silver or tin capsules, respectively, and either acidified with 1 mol L^{-1} HCl and dried at 50 °C overnight in order to measure POC/N$_{ST}$ or kept unacidified for TPC/N$_{ST}$ analysis. Duplicates were measured on a CN analyzer (Euro EA-CN, HEKAtech GmbH, Wegberg, Germany) according to Sharp (1974). PIC$_{ST}$ concentrations were calculated from the difference of TPC$_{ST}$ to POC$_{ST}$. BSi$_{ST}$ and POP$_{ST}$ concentrations were measured spectrophotometrically according to Hansen and Koroleff (1999), after subsampling ~ 2 mg of the sediment. Prior to that, POP samples were pressure-cooked in 40 mL of deionized water including an oxidizing agent (Oxisolv, Merck).

2.3.2 Particle sinking velocities

Sinking velocities (SVs) of sediment trap material were determined every 2 d by means of video microscopy. A repurposed FlowCam (Fluid Imaging Technologies Inc., Scarborough, United States) was used to capture images of particles during gravitational sinking. A vertically mounted sinking chamber (cuvette with the dimensions $10 \times 10 \times 350$ mm) was placed in front of the camera (see Bach et al., 2012, for technical details). Sediment subsamples were inspected visually and diluted (with filtered seawater < 0.2 µm) in a small cup according to their particle density ($1 : 1$–$1 : 40$). Diluted samples were loaded into the sinking chamber by a pipette and pileus ball attached on top. Fluid advection within the sinking chamber could be ruled out by ensuring air tightness. Measurements were carried out at in situ temperatures (~ 22 °C), and additional ventilation minimized convection within the sinking chamber. Particles between 25–1000 µm were identified with $2\times$ magnification and 20 frames per second, and their sinking velocities were calculated by applying a linear regression to the vertical position against time. Several optical parameters allowed the identification of the multiple frames of a single particle during gravitational sinking, and calculations in the MATLAB script (version R2021b; provided by Bach et al., 2012; see "Evaluation of sinking velocities") were adjusted to the more recent version of the FlowCam 8000. These were corrected for temperature differences during measurements and for wall effects of the sinking chamber following Ristow (1997). Partially captured par-

ticles or those out of focus were excluded within the MATLAB script, prior to the SV calculation. Measurements were run for 20 min, and subsequent data analysis was carried out with the programming software R (R Core Team, 2021) using the package *tidyverse* (Wickham et al., 2019) in RStudio (Version 4.1.1.). It is important to note that measured particle size spectra are derived from ex situ measurements and thus do not accurately represent the in situ size distribution. Nevertheless, they allowed following in situ particle dynamics due to, for example, aggregation, packing, or grazing closely.

2.3.3 Remineralization rates of sinking particles

Carbon-specific remineralization rates were determined every 4–6 d. During the water column sampling, four replicate and three control bottles for each mesocosm were filled headspace-free. Upon arrival in the temperature-controlled lab (in situ temperature of the respective day), the respiration bottles were acclimatized in a water bath for 1 h. Depending on particle density, 0.5–10 mL of homogenized sediment subsample of the respective mesocosm was slowly injected into four replicated bottles. Control bottles ($n = 3$) did not receive any sediment. Subsequently, all bottles were incubated in the dark on a plankton wheel (~ 1 rpm) for 22–26 h. Non-invasive O$_2$ measurements were carried out at regular intervals (approx. every 4 h) using a fiber-optical measurement device (Fibox4 Trace, PreSens – Precision Sensing GmbH, Regensburg, Germany) and PSt3 sensor spots (PreSens) mounted to the inside walls of the incubated bottles. Corrections for atmospheric pressure and temperature (using a dummy bottle) were automatically done by the Fibox4. The Fibox4 salinity correction was set to the mean mesocosm salinity of the respective day (CTD measurement).

Incubations were terminated with the collection of POC (sediment + suspended) within the bottles on pre-combusted glass fiber filters (0.7 µm, Whatman). The carbon content analysis was carried out as described for POC$_{WC}$ (see Sect. 2.3.4). The carbon-specific remineralization rate of sedimented particulate matter (C$_{remin}$ in d^{-1}) was calculated as follows:

$$C_{remin} = \frac{(r \times RQ)}{(POC + r \times RQ \times \Delta t)}. \tag{1}$$

The O$_2$ consumption rate (r in µmol O$_2$ L^{-1} d^{-1}) was normalized to the POC (µmol C L^{-1}) contained within the bottles, which was corrected for the duration of the incubation (Δt in d). The respiration quotient (RQ in mol C mol O$_2^{-1}$) equalled 1, since the consumption of O$_2$ is commonly as-

sumed to be equal to the production of CO_2 during organic matter turnover (Ploug and Grossart, 2000; Iversen and Ploug, 2013; Bach et al., 2019c). To differentiate the influence of sediment respiration from ambient seawater O_2 consumption, C_{remin} was corrected for the mean blank bottle values.

2.3.4 Phytoplankton biomass, abundances, and water column stoichiometry

Subsampling for TPC/N_{WC}, POC/N_{WC}, and Chl a was achieved by filtering the water column samples onto separate pre-combusted glass fiber filters (0.7 µm, Whatman). To remove inorganic carbon, POC/N_{WC} filters were acidified for ~ 30 s using $1 \, mol \, L^{-1}$ HCl. Additionally, unacidified filters for TPC/N_{WC} were collected. Both filter types were stored in pre-combusted glass petri dishes and dried at 60 °C overnight. All filters were packed into tin cups ($8 \times 8 \times 15$ mm, LabNeed GmbH, Nidderau, Germany), stored in a desiccator and transported back to Kiel. Carbon content of filters was determined with a CN analyzer (Euro EA-CN, HEKAtech) as described for the sediment trap samples. PIC_{WC} concentrations were calculated as described for the sediment trap samples.

Chl a was extracted in plastic vials using acetone (90 %) and subsequent homogenization in a cell mill with glass beads (5 min; Vibrogen, Berlin, Germany). The suspension was centrifuged (10 min, 800 g, 4 °C; Universal 320, Hettich, Bäch, Germany), and the resulting supernatant was analyzed with a fluorometer (TURNER Trilogy, Turner Designs, San Jose, United States) according to Welschmeyer (1994). Spinach Chl a extract (Sigma-Aldrich, St. Louis, United States) was used to calibrate the fluorometer (Strickland and Parsons, 1972).

Phyto- and microzooplankton abundances were determined by microscope from bulk water samples according to Utermöhl (1958) after fixating in a basic Lugol's solution and letting samples settle in a chamber for 24 h.

2.3.5 Carbonate chemistry and nutrient concentrations

TA and DIC samples were taken with an overflow of ~ 2 times the final sampling volume, carefully avoiding air inclusion. Within 12 h, samples were measured at room temperature. To remove PIC_{WC}, both TA and DIC samples were filtered (0.2 µm, Whatman). TA was determined in duplicate with hydrochloric acid (0.05 M) in a two-stage open-cell potentiometric titrator (Compact Titrosampler 862, Metrohm, Munich, Germany).

DIC was determined in triplicate by infrared absorption using an AIRICA system (MARIANDA, Kiel, Germany) with a differential gas analyzer (LI-7000, LI-COR Biosciences GmbH, Bad Homburg, Germany). Values of DIC and TA were calibrated against certified reference material (batch nos. 143, 190; Dickson, 2010). Further car-

bonate chemistry parameters were calculated with the Excel macro *CO2SYS* (Pierrot et al., 2011) using the (water-column-averaged) temperature and salinity CTD measurements for correction. The carbonate dissociation constants (K_1 and K_2) from Lueker et al. (2000) were chosen.

Dissolved inorganic nutrient concentrations ($NO_3^- + NO_2^-$, PO_4^{3-}, $Si(OH)_4$) were measured spectrophotometrically on a five-channel continuous flow analyzer (QuAAtro AutoAnalyzer, SEAL Analytical Inc., Mequon, United States) with a fluorescence detector (FP-2020, JASCO, Pfungstadt, Germany). Approaches of Murphy and Riley (1962), Mullin and Riley (1955), and Morris and Riley (1963) were followed for all colorimetric methods, and refractive index correction was done according to Coverly et al. (2012).

2.4 Statistical analysis

Linear mixed-effects models were used to assess the OAE effect on the different export-related response variables. OAE was set as a continuous fixed effect, day as a categorical fixed effect, and mesocosm as a random effect (*nlme* package; Pinheiro et al., 2022). The interaction term of OAE × day was set as an additional fixed effect to test how the OAE effect changed over time. For all analyses, assumptions were checked using residual-vs.-fitted plots (homogeneity of variances and Q–Q plots; normality of residuals; *performance* package; Lüdecke et al., 2021). Their violation was corrected for by data transformations (Table S3). All analyses were conducted at a significance level of $\alpha = 0.05$ using R (R Core Team, 2021). Additionally, averages over experimental phases were calculated for specific response variables and their dependency on OAE tested using simple linear regressions. The highest OAE level (ΔTA_{2400}) was excluded from all statistical analyses as it developed considerable abiotic precipitation, which interfered with the interpretation of the OAE's effect on the biological pump. Welch's t test on TA between two phases of the experiment (Days 4–17 vs. Days 19–33; Table S2) confirmed its standing as an extreme outlier.

3 Results

3.1 Achieved alkalinity enhancement and plankton community biomass

We successfully applied OAE to the mesocosms, and target alkalinity levels remained stable throughout the experiment (Fig. 1a). An exception was the highest OAE level, which only remained stable until Day 17, after which ΔTA_{2400} continuously declined, dropping below ΔTA_{2100} on Day 33. This alkalinity consumption was induced by abiotic calcium carbonate precipitation (see Sect. 4.2). Phytoplankton biomass approximated by chlorophyll a and particulate organic carbon in the water column (POC_{WC}) did not

change with respect to OAE (Fig. 1b, c; Table S4). It remained low in the first half of the experiment (Days 3–21; Fig. S3), after which chlorophyll a and POC_{WC} concentrations unexpectedly increased in some mesocosms (ΔTA_{600}, ΔTA_{900}, ΔTA_{1500}, and ΔTA_{1800}). These blooms occurred despite oligotrophic conditions throughout the entire experiment (Fig. S2) and were likely caused by a mixotrophic haptophyte species of *Chrysochromulina* spp. (Xin et al., 2025).

3.2 Organic matter fluxes and stoichiometry

Ocean alkalinity enhancement did not influence the magnitude of the particulate organic carbon flux (POC_{ST}): neither the cumulated POC_{ST} over the entire experiment, nor on a daily basis (Table S3a). Irrespective of OAE, carbon export fluxes decreased over time (Fig. 2a). Higher initial fluxes (Days 7 and 9) reflected the decreasing phytoplankton biomass of preceding days, on which an average 8-fold decrease was visible until Day 27. Other major elemental fluxes (PON_{ST}, POP_{ST}, and BSi_{ST}) were likewise not influenced by OAE (Fig. 2c, e, f; Table S3i, j, k) and had similar temporal trends to POC fluxes (Fig. S4b, c, d). Whether the export of the major elements was affected within the blooming mesocosms (ΔTA_{600}, ΔTA_{900}, ΔTA_{1500}, and ΔTA_{1800}; Fig. S4) remains unclear, yet the influence of wall cleaning is apparent from Day 17 onwards, as wall growth intensified. Carbon-to-nitrogen ratios ($POC_{ST} : PON_{ST}$) of exported matter did not change with respect to OAE (Fig. 2d). The stoichiometric composition stayed constant throughout the experiment (Table S3b) and generally well above the canonical Redfield ratio of 6.6 (Fig. S4a). Likewise, opal ballasting ($BSi_{ST} : POC_{ST}$) was unaffected by OAE (Figs. 2g, S4e; Table S3l).

3.3 Particle sinking velocities and remineralization rates

OAE had no effect on either particle sinking velocities or remineralization rates of sinking material, leaving the potential flux attenuation with depth unchanged (Fig. 3a, c and Table S3f, m). Particle sinking velocities (SVs) were generally low (10–35 $m\,d^{-1}$) and did not respond to OAE: neither overall (Fig. 3a), nor for specific particle size classes (Fig. S5). Sinking velocities of ΔTA_{2400} exceeded those of all other alkalinity levels from Day 15 onwards and are expected to be caused by increased ballasting due to the abiotically precipitated carbonate mineral (see Sect. 4.2). Remineralization rates (C_{remin}) did not change under OAE (Fig. 3c; Table S3f), staying relatively constant with carbon turnover, varying between 7 and 18 % d^{-1} (Fig. 3c). Noticeably higher remineralization rates of ΔTA_{2400} on Days 27 and 33 were not paralleled by higher O_2 consumption rates across incubations (Fig. S7) and were probably caused by an unresolved sample processing error due to the abiotic precipitation (see Sect. 4.2).

3.4 Abiotic precipitation, inorganic carbon fluxes, and carbonate ballasting

Particulate inorganic carbon export (PIC_{ST}) and carbonate ballasting ($PIC_{ST} : POC_{ST}$) increased under OAE (Figs. 4a, S6a; Table S3g, h). Between Days 19 and 31, average PIC_{ST} fluxes almost tripled from ambient seawater alkalinity to ΔTA_{2100} (Fig. 4b), while carbonate ballasting more than doubled (Fig. S6b). Additionally, the PIC_{ST} flux in ΔTA_{2400} exceeded those of all other alkalinity levels from Day 17 onwards, and pCO_2 was highest (e.g., 541 µatm on Day 33). High PIC_{ST} fluxes coincided with a white precipitate (Fig. S8d), especially apparent on the walls of the mesocosm ΔTA_{2400}, which upon wall cleaning sank to the sediment traps. This direct consequence of the abiotic precipitation increased ballasting material within the sediment trap and thus particle sinking velocities (Fig. 4c). Sinking velocities in the medium (100–250 µm) particle size class increased by 30 $m\,d^{-1}$ with every mol mol^{-1} in $PIC_{ST} : POC_{ST}$. Although less discernible, particles in the smallest size range (25–100 µm) increased by 18.10 $m\,d^{-1}$ per increment of $PIC_{ST} : POC_{ST}$ (note marginally significance: $p = 0.065$; Table S4). While screenshots from the FlowCam indicated that larger particles were actually ballasted (distinct and dark particles in aggregates; Fig. 4d), solitary precipitates were also visible. It appears that both ballasting of larger aggregates within the sediment trap and solitary precipitates increased the measured particle sinking velocities across all sizes (Fig. S5).

4 Discussion

4.1 Particle export by the plankton community

Ocean alkalinity enhancement did not influence the biotically driven flux of major elements (C, N, P, Si), stoichiometric ratios, or potential depth attenuation (particle sinking velocities and remineralization rates). These findings are in line with the lack of a detectable effect on plankton community composition or water column biogeochemistry during our experiment (Paul et al., 2024). Yet the sporadically occurring blooms within some mesocosms (ΔTA_{600}, ΔTA_{900}, ΔTA_{1500}, and ΔTA_{1800}) were unexpected, considering the oligotrophic conditions within our mesocosms. In general, the community displayed a typical assemblage of open-ocean gyres (Dai et al., 2023) and was dominated by picoeukaryotes (e.g., *Synechococcus*) and to lesser extent by diatoms (Xin et al., 2025). The bloom-forming species was identified by Xin et al. (2025) as *Chrysochromulina* spp., a non-calcifying haptophyte species with a cyanobacterial endosymbiont capable of nitrogen fixation (UCYN-A, Suzuki et al., 2021), allowing them to thrive in the otherwise nutrient-depleted mesocosm. Additionally, potential responses of calcifiers to OAE (due to an increase in Ω and pH) were either absent or not detected due to their low abun-
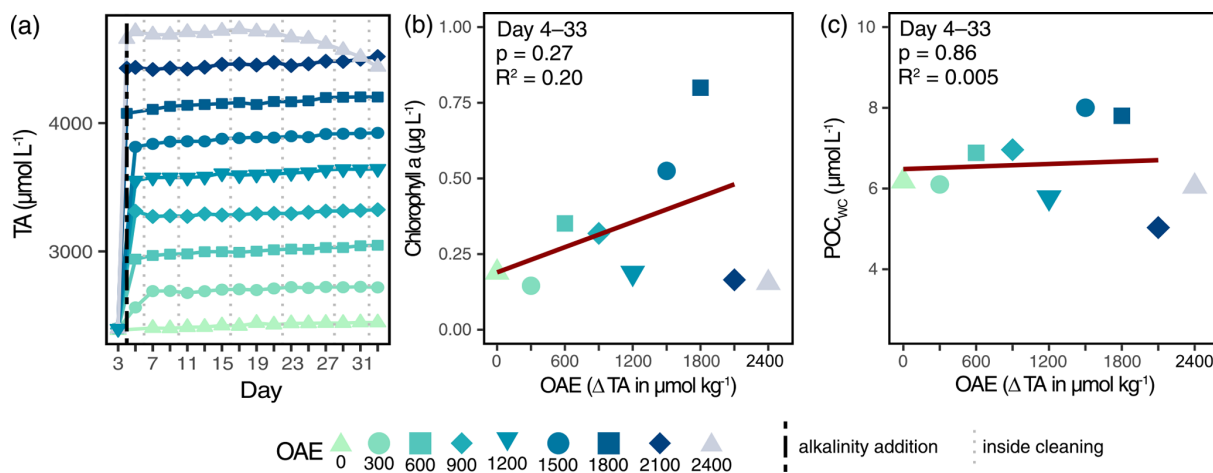
Figure 1. Abiotic and biotic responses of the water column to the application of OAE. Achieved alkalinity enhancement and its stability over time **(a)**. The vertical black line indicates the alkalinity addition and the grey lines the inside cleaning of the mesocosm walls. Chlorophyll *a* **(b)** and carbon biomass **(c)** of the plankton community. Averages over the treatment period are employed in linear regressions.
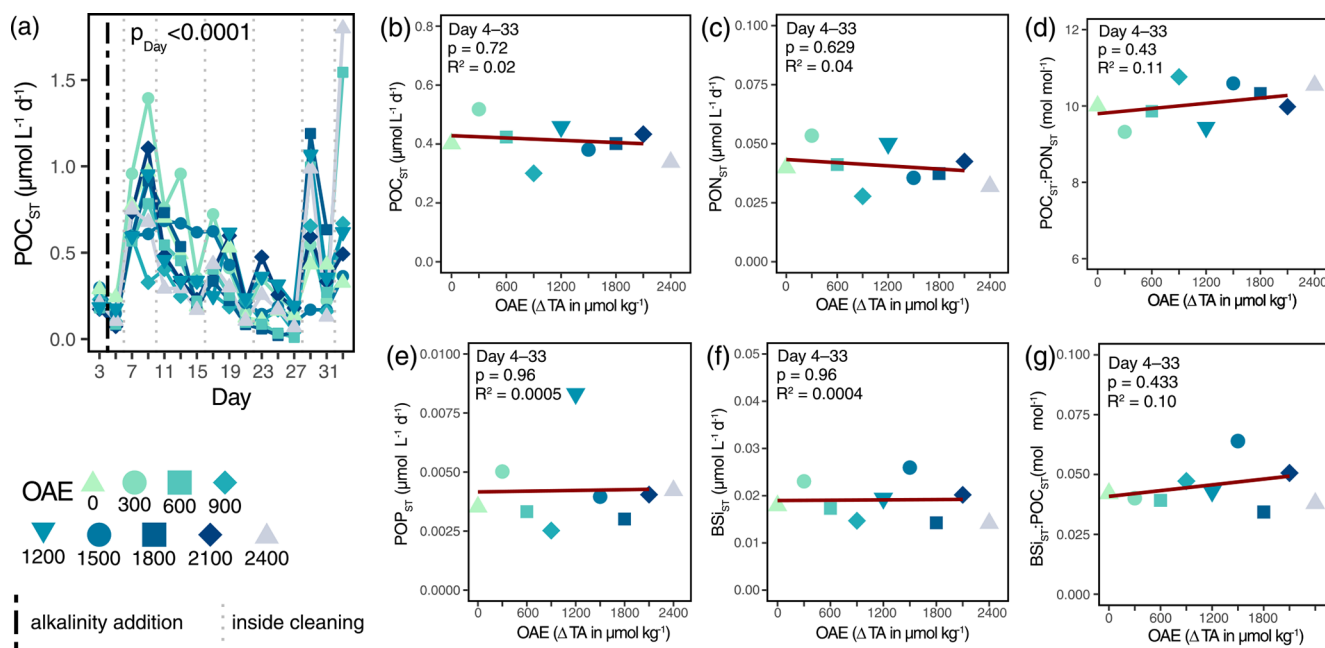

Figure 2. Organic matter fluxes and stoichiometry under the application of OAE. Organic carbon flux and its response to OAE over time **(a)** and averaged across the treatment period **(b)**. The p value in **(a)** represents the output of linear mixed-effects model (Table S3a). The vertical black line indicates the alkalinity addition and the grey lines the inside cleaning of the mesocosm walls. Other major elemental fluxes (PON_{ST}, POP_{ST}, BSi_{ST}) in response to OAE averaged over the treatment period **(c, e, f)**. Quality and ballasting of the export flux ($POC_{ST} : PON_{ST}$, $BSi_{ST} : POC_{ST}$) averaged over the treatment period employed as linear regressions **(d, g)**.

dances (Fig. S8a–c), limiting conclusions of their influence on carbon export. This contrasted theoretical expectations (Jokiel, 2011; Monteiro et al., 2016; Bach, 2015), and we restrict this section to a general discussion of what might have caused the absence or disappearance of calcifying organisms during our experiment. Calcifying organisms are scarce in nutrient-poor seasons around the Canary Islands (Sprengel et al., 2002), underlining that a relevant seeding of meso-

cosms, similar to previous studies (Bach et al., 2017; Taucher et al., 2017; Bach et al., 2019c; Ortiz et al., 2022), might not have occurred. Additionally, Ortiz et al. (2022) only reported a significant contribution of calcifiers to the phytoplankton community upon repeated deep-water addition, implying that their potential competitive advantages under OAE (resource allocation towards growth and metabolic processes compared to calcification) could not be thoroughly expressed
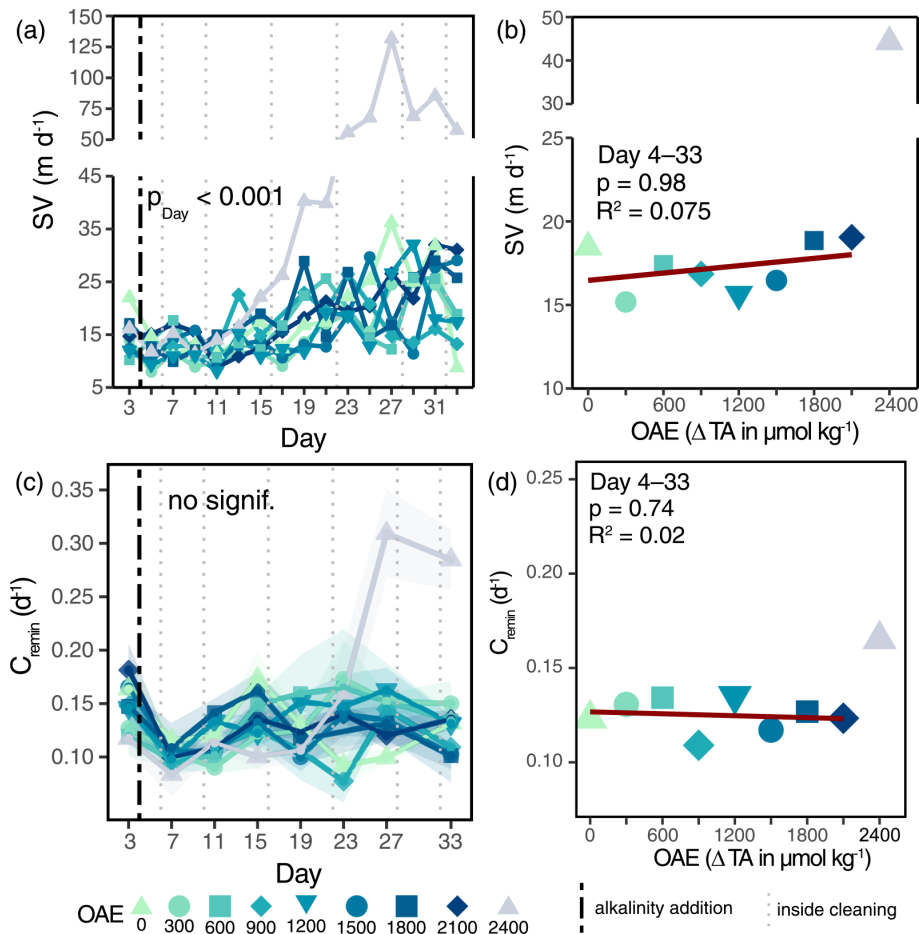
Figure 3. Depth attenuation of the organic matter flux under the application of OAE. Development of average particle sinking velocities under OAE over time **(a)** and as averages over the treatment period **(b)**. Carbon-specific remineralization rates **(c)** and averages under OAE **(d)**. Shaded areas in **(c)** indicate standard deviations of measurements ($n_{min} = 3$). p values in **(a)** and **(c)** represent the output of linear mixed-effects models (Table S3f, m). The vertical black line indicates the alkalinity addition and the grey lines the inside cleaning of the mesocosm walls **(a, c)**.

under the nutrient-deprived conditions of our study. In a recent alkalinity enhancement study, Gately et al. (2023) came to similar conclusions, claiming that nutrient concentrations and ratios, compared to alkalinity, may be a stronger driver governing phytoplankton community composition. Hence, the nutrient-deprived ecosystem, in suite with the deliberately small carbonate chemistry perturbations (only changing pH by up to 0.2 units), allowed us to assess this least impactful OAE scenario. This least impactful scenario did not translate to detectable effects on calcifiers nor the remaining phytoplankton community (Xin et al., 2025) and the elemental fluxes they drive. This is consistent with previous ocean acidification studies, which found pronounced responses only at larger pH differences and during blooms (Stange et al., 2018; Taucher et al., 2017). Therein, particle fluxes only changed for a pH decrease of 0.5 units and upon adding nutrient-rich deep water to the oligotrophic system, which stimulated considerable primary production, in contrast to our study as in-

ferred from unchanged water column chlorophyll a and POC concentrations.

Carbon-to-nitrogen ratios of exported matter remained unchanged under OAE and are in the same range as ratios found during previous mesocosm studies (Stange et al., 2018; Bach et al., 2019c; Baumann et al., 2021) and for natural unalkalized export fluxes in the Canary Island region (Freudenthal et al., 2001). Our findings contrast Taucher et al. (2021), where ocean acidification altered carbon-to-nitrogen ratios due to varying heterotrophic respiration. While pH-dependent microbial N-cycle processes theoretically could affect these ratios (Fumasoli et al., 2017; Pommerening-Röser and Koops, 2005; Beman et al., 2011), we want to note that observed optimal pH for these processes usually falls below the modest pH range implemented in this study. Instead, we attribute the stability of carbon-to-nitrogen ratios in our study to the nutrient-deprived conditions in combination with small pH changes (compared to Taucher et al.,
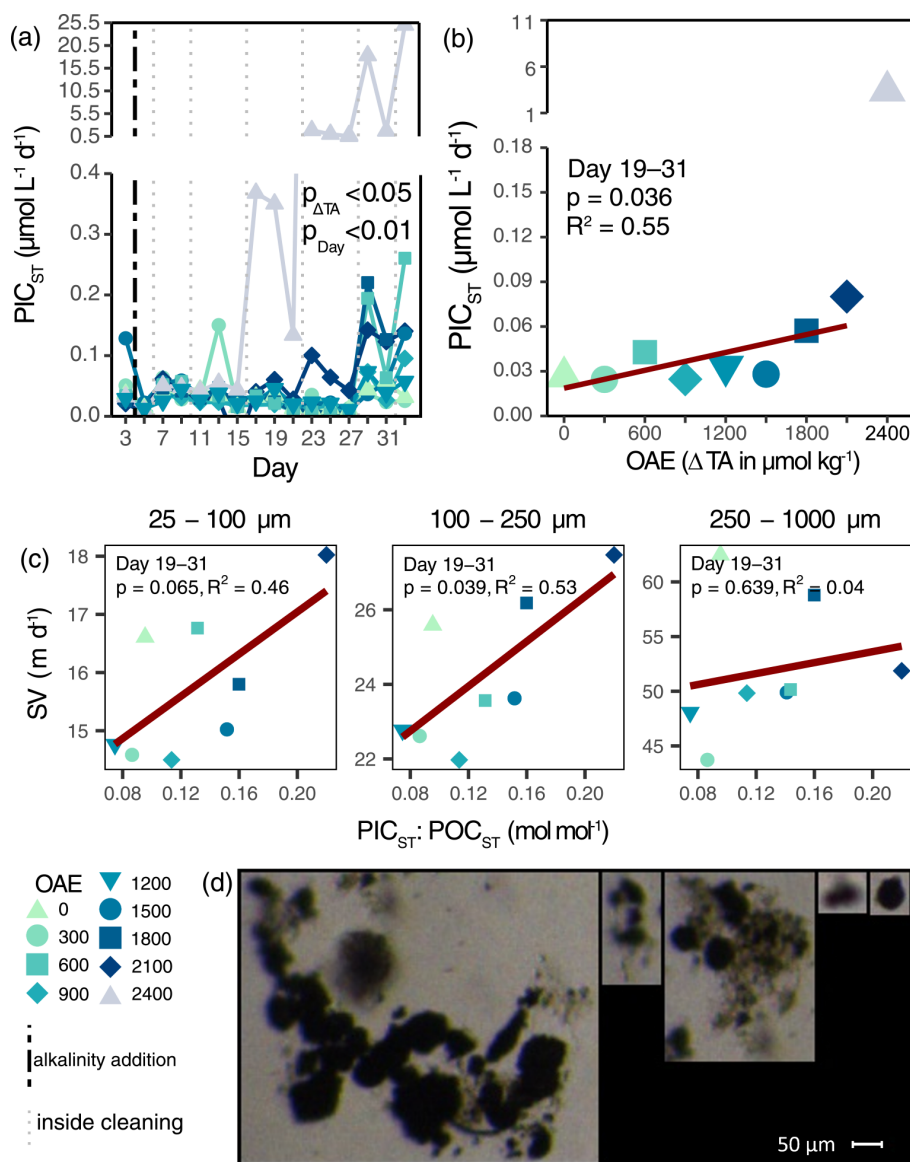
Figure 4. Inorganic export flux and carbonate ballasting. Inorganic carbon export and its response to OAE over time **(a)** and as averaged over the treatment period **(b)**. p value in **(a)** represents the output of linear mixed-effects model (Table S3g). The vertical black line indicates the alkalinity addition and the grey lines the inside cleaning of the mesocosm walls. Average particle sinking velocities of different size classes and their response to carbonate ballasting during the phase of abiotic precipitation **(c)**. Selection of FlowCam screenshots of sediment trap material on Day 23 displaying carbonate ballasting of aggregates and individual carbonate precipitates **(d)**.

2021), once again mirroring a lack of a detectable community effect under OAE.

While there is a chance that OAE effects might have emerged with longer experiment duration, added alkalinity for different application scenarios (e.g., in the wake of ships) is expected to dilute on timescales considerably shorter than our study length (Byrne et al., 1988). This gives further confidence that the particle fluxes, their properties, and therefore the potential to sequester carbon via the biological pump would remain unimpeded in the oligotrophic open ocean under CO_2 pre-equilibrated OAE.

Other approaches, however, let pCO_2 equilibrate post-alkalinity application and might be conducted in nutrient-rich ecosystems. Carbonate chemistry perturbations thus can be more severe during OAE, and responses of plankton communities thereto might even be amplified during blooms, ultimately altering the biological carbon pump. For instance, non-equilibrated OAE could lead to CO_2 limitation in phytoplankton, which could hamper primary and subsequently biomass production (Bach et al., 2020; Zagarese et al., 2021; Riebesell et al., 1993) with the potential to decrease export production. Non-equilibrated alkalinity enhancement also

entails a stronger pH change at which effects absent at milder perturbations might eventually emerge, analogous to several ocean acidification studies (Stange et al., 2018; Taucher et al., 2017). A lesson from strong pH perturbations under ocean acidification is that bacterial activity might increase (Piontek et al., 2010; Endres et al., 2014) such that a decrease under non-equilibrated OAE is conceivable. This would impair nutrient recycling and release in the surface ocean (Karthäuser et al., 2021; Cabanes et al., 2017), eventually shortening the bloom period (Böckmann et al., 2021; Sarthou et al., 2008; Cherabier and Ferrière, 2022) and consequently decreasing the potential export production throughout a season (Iversen, 2023). On the other hand, copepods have been shown to increase their feeding rates in response to elevated pH (Li et al., 2008). Increased ingestion and egestion rates are thus conceivable under OAE, potentially leading to a larger quantity of fast-sinking fecal pellets (Stukel et al., 2011; Le Moigne et al., 2016), which eventually would decrease the depth attenuation of the export flux (Guidi et al., 2015).

While oligotrophic conditions in the Canary Island region are prevailing, eddy-induced nutrient upwelling is not uncommon (Arístegui et al., 1997; Basterretxea et al., 2002). Additionally, application of OAE is also considered in nutrient-rich coastal zones or upwelling areas, since it would require less technical effort compared to open-ocean applications, as represented by our study (Bach et al., 2019a). Thus, alkalinity-enhanced water parcels may experience blooms. In parallel with several ocean acidification studies, the blooming communities' sensitivity to the concomitant carbonate chemistry perturbations can alter particle fluxes and emissions of climate-relevant trace gases (Bach et al., 2016; Webb et al., 2016; Riebesell et al., 2017; Stange et al., 2018; Taucher et al., 2017). Thus, feedbacks of OAE on the biological carbon pump may be diverse, necessitating research on different application approaches and across nutrient regimes in further multi-trophic ecosystem studies.

4.2 Abiotic precipitation and alkalinity leakage

Particulate inorganic carbon fluxes increased with alkalinity enhancement, an effect that has become more prominent with time. Yet observed fluxes were apparently not driven by biotic production, given the low abundances of calcifying organisms during our mesocosm experiment (Xin et al., 2025; Fig. S8). Instead, the increased carbonate fluxes and the alkalinity loss observed in ΔTA_{2400} resulted from abiotic precipitation. This process was not unique to the highest treatment, as carbonate fluxes and water column ballasting ratios increased at lower treatment levels (ΔTA_{1800} and ΔTA_{2100}) as well (Paul et al., 2024).

Such abiotic precipitation under OAE has been observed previously (Moras et al., 2022; Griffioen, 2017; Subhas et al., 2022) and is known to occur for carbonate saturation states well below the threshold for spontaneous precipitation (Table S1: $\Omega_{Ar} = 10.01$ and $\Omega_{Ca} = 15.24$, compared to $\Omega_{Ar} = 12.5$–13.5; Morse and He, 1993). In fact, Wurgaft et al. (2021) noted carbonate precipitation at alkalinity concentrations close to our control treatment. The process can be initiated by the presence of suitable precipitation nuclei, which has been noted in the field (Wurgaft et al., 2021) and during separate short-term incubations with mesocosm water during our campaign (Hartmann et al., 2023). Yet it is important to note that thresholds for spontaneous precipitation remain poorly constrained in natural ecosystems. This arises primarily from uncertainties regarding the influence of colloids and organic materials as precipitation nuclei, as well as diverse ranges of temperature and salinity, both affecting the kinetics and thermodynamics of secondary precipitation (Moras et al., 2022; Hartmann et al., 2023, 2013; Marion et al., 2009). However, artificial surfaces for precipitation were present through the mesocosm walls, which in combination with the perturbed carbonate chemistry may explain the observed precipitation at our higher alkalinity levels. Thus, a large portion of the formed PIC could be regarded an experimental artifact, which needs to be considered when interpreting particle sinking velocities. The majority of precipitated carbonates slid down the mesocosm walls upon cleaning so that most ballasting likely occurred through aggregation within the sediment trap where both PIC from the walls and POC from the water column accumulated. Given this spatial separation of inorganic and organic carbon flux production, it seems improbable that significant ballasting of aggregates and increase of sinking velocities occurred through scavenging of particles within the water column. However, being a strong predictor of particle sinking velocities (Honjo et al., 2008; Armstrong et al., 2001; Bach et al., 2016), carbonate ballasting yielded the prominent positive relation to particle sinking velocities seen in Fig. 4c, in contrast to OAE itself (Fig. 3b). The plankton community structure, likewise a strong predictor of particle sinking velocities (Bach et al., 2019c, 2016), did not display a response to OAE. Instead its natural variability among mesocosms likely obscured the detection of significant changes in sinking velocities with OAE. As such, alkalinity itself yielded weaker relations to particle sinking velocities, as compared to the experimental artifact of enhanced carbonate ballasting through abiotic precipitation. However, we still want to conclude that abiotic precipitation likely did not affect sinking velocities within the water column such that the increase over time could not have actually affected the potential depth attenuation of the biological pump during our experiment. Additionally, the magnitude of PIC formation in open-ocean settings would likely be substantially lower than during our study, since suitable precipitation nuclei are mostly scarce.

Abiotic precipitation has also been noted for suspended particles (Ferderer et al., 2022; Hartmann et al., 2023). It is thus imaginable not only for coastal ecosystems with large surface areas (e.g., seagrass meadows), but also for the open ocean, given the periodic presence of precipitation nuclei through, for example, dust deposition. Although OAE should

be maintained well outside a TA range where such precipitation might occur, it is worthwhile to consider its potential implications on particle fluxes should such a worst-case scenario arise. Carbonate ballasting from OAE-induced precipitates is likely to behave differently, as compared to, for example, coccolithophore-derived ballasting. Opposing abiotic precipitates, biological carbonate-containing particles also include lighter organic matter, which exerts less ballast on sinking aggregates. In addition, the abiotic PIC particles were considerably larger ($50\,\mu m$) than, for example, coccolithophore-derived particles (Jordan, 2009; Rothwell, 2016). Larger particles have been shown to be scavenged and ballast sinking aggregates preferably (Puig et al., 2013; McCave, 1983). Abiotic precipitates are thus not only heavier at similar size, but potentially also larger, exerting more ballasting potential than many biologically derived carbonates, and may substantially alter open-ocean export dynamics under such adverse OAE scenarios. The onset of abiotic carbonate precipitation would also oppose the desired effects of ocean alkalinity enhancement. Given the supersaturation of surface waters with respect to calcium carbonate (Mucci, 1983), a significant export of the precipitated carbonate mineral is conceivable, transporting alkalinity to waters out of contact with the atmosphere. Such calcium carbonate precipitation releases CO_2 (Zeebe and Wolf-Gladrow, 2010), further decreasing OAE's efficacy to store atmospheric carbon. Additionally, abiotic carbonate precipitation may sustain itself to a point where alkalinity drops below initial background concentrations (Moras et al., 2022; Brečević and Nielsen, 1989; Hartmann et al., 2023), eventually turning alkalinity-enhanced waters into a source rather than a sink for CO_2. To conclude, our concerns of raising alkalinity to levels inducing precipitation extend beyond the CO_2 released upon carbonate precipitation but to potential adverse effects on the biological carbon pump as well.

5 Conclusions

Our findings suggest that particle fluxes by subtropical pelagic communities are insensitive to CO_2 pre-equilibrated OAE, leaving carbon sequestration via the biological pump unimpeded by this most optimistic approach. It will be paramount to test effects on the magnitude and quality of export fluxes across nutrient-richer ecosystems and for non-equilibrated OAE approaches. Undesired abiotic carbonate precipitation may induce alkalinity consumption and requires close monitoring. It may not only decrease OAE's efficacy to store atmospheric carbon, but potentially also alters the biological pump's capability to sequester atmospheric CO_2. Ultimately, our results are a promising starting point for further assessments on this carbon dioxide removal technology, prompting the necessity to holistically consider biotic and abiotic impacts, before drawing sound conclusions on the safe applicability of OAE.

Review statement. This paper was edited by Jaime Palter and reviewed by two anonymous referees.

References

Arístegui, J., Tett, P., Hernández-Guerra, A., Basterretxea, G., Montero, M. F., Wild, K., Sangrá, P., Hernández-Leon, S., Canton, M., García-Braun, J. A., Pacheco, M., and Barton, E. D.: The influence of island-generated eddies on chlorophyll distribution: a study of mesoscale variation around Gran Canaria, Deep-Sea Res. Pt. I, 44, 71–96, https://doi.org/10.1016/S0967-0637(96)00093-3, 1997.

Armstrong, R. A., Lee, C., Hedges, J. I., Honjo, S., and Wakeham, S. G.: A new, mechanistic model for organic carbon fluxes in the ocean based on the quantitative association of POC with ballast minerals, Deep-Sea Res. Pt. II, 49, 219–236, https://doi.org/10.1016/S0967-0645(01)00101-1, 2001.

Bach, L. T.: Reconsidering the role of carbonate ion concentration in calcification by marine organisms, Biogeosciences, 12, 4939–4951, https://doi.org/10.5194/bg-12-4939-2015, 2015.

Bach, L. T., Riebesell, U., Sett, S., Febiri, S., Rzepka, P., and Schulz, K. G.: An approach for particle sinking velocity measurements in the 3–400 µm size range and considerations on the effect of temperature on sinking rates, Mar. Biol., 159, 1853–1864, https://doi.org/10.1007/s00227-012-1945-2, 2012.

Bach, L. T., Boxhammer, T., Larsen, A., Hildebrandt, N., Schulz, K. G., and Riebesell, U.: Influence of plankton community structure on the sinking velocity of marine aggregates, Global Biogeochem. Cy., 30, 1145–1165, https://doi.org/10.1029/2019GB006256, 2016.

Bach, L. T., Alvarez-Fernandez, S., Hornick, T., Stuhr, A., and Riebesell, U.: Simulated ocean acidification reveals winners and losers in coastal phytoplankton, PLOS ONE 12, e0188198, https://doi.org/10.1371/journal.pone.0188198, 2017.

Bach, L. T., Gill, S. J., Rickaby, R. E. M., Gore, S., and Renforth, P.: CO$_2$ Removal With Enhanced Weathering and Ocean Alkalinity Enhancement, Frontiers in Climate, 1, 7, https://doi.org/10.3389/fclim.2019.00007, 2019a.

Bach, L. T., Hernández-Hernández, N., Taucher, J., Spisla, C., Sforna, C., Riebesell, U., and Arístegui, J.: Effects of Elevated CO$_2$ on a Natural Diatom Community in the Subtropical NE Atlantic, Front. Mar. Sci., 6, 320, https://doi.org/10.3389/fmars.2019.00075, 2019b.

Bach, L. T., Stange, P., Taucher, J., Achterberg, E. P., Algueró-Muñiz, M., Horn, H., Esposito, M., and Riebesell, U.: The Influence of Plankton Community Structure on Sinking Velocity and Remineralization Rate of Ma-

rine Aggregates, Global Biogeochem. Cy., 33, 971–994, https://doi.org/10.1029/2019GB006256, 2019c.

Bach, L. T., Paul, A. J., Boxhammer, T., von der Esch, E., Graco, M., Schulz, K. G., Achterberg, E., Aguayo, P., Arístegui, J., Ayón, P., Baños, I., Bernales, A., Boegeholz, A. S., Chavez, F., Chavez, G., Chen, S.-M., Doering, K., Filella, A., Fischer, M., Grasse, P., Haunost, M., Hennke, J., Hernández-Hernández, N., Hopwood, M., Igarza, M., Kalter, V., Kittu, L., Kohnert, P., Ledesma, J., Lieberum, C., Lischka, S., Löscher, C., Ludwig, A., Mendoza, U., Meyer, J., Meyer, J., Minutolo, F., Ortiz Cortes, J., Piiparinen, J., Sforna, C., Spilling, K., Sanchez, S., Spisla, C., Sswat, M., Zavala Moreira, M., and Riebesell, U.: Factors controlling plankton community production, export flux, and particulate matter stoichiometry in the coastal upwelling system off Peru, Biogeosciences, 17, 4831–4852, https://doi.org/10.5194/bg-17-4831-2020, 2020.

Barton, E. D., Arìstegui, J., Tett, P., Cantón, M., Garcìa-Braun, J., Hernández-León, S., Nykjaer, L., Almeida, C., Almunia, J., Ballesteros, S., Basterretxea, G., Escánez, J., Garcìa-Weill, L., Hernández-Guerra, A., López-Laatzen, F., Molina, R., Montero, M. F., Navarro-Pérez, E., Rodrìguez, J. M., van Lenning, K., Vélez, H., and Wild, K.: The transition zone of the Canary Current upwelling region, Prog. Oceanogr., 41, 455–504, https://doi.org/10.1016/S0079-6611(98)00023-8, 1998.

Basterretxea, G., Barton, E. D., Tett, P., Sangrá, P., Navarro-Perez, E., and Arı´stegui, J.: Eddy and deep chlorophyl maximum response to wind-shear in the lee of Gran Canaria, Deep-Sea Res. Pt. I, 49, 1087–1101, https://doi.org/10.1016/S0967-0637(02)00009-2, 2002.

Baumann, M., Taucher, J., Paul, A. J., Heinemann, M., Vanharanta, M., Bach, L. T., Spilling, K., Ortiz, J., Arístegui, J., Hernández-Hernández, N., Baños, I., and Riebesell, U.: Effect of Intensity and Mode of Artificial Upwelling on Particle Flux and Carbon Export, Frontiers in Marine Science, 8, 742142, https://doi.org/10.3389/fmars.2021.742142, 2021.

Beman, J. M., Chow, C.-E., King, A. L., Feng, Y., Fuhrman, J. A., Andersson, A., Bates, N. R., Popp, B. N., and Hutchins, D. A.: Global declines in oceanic nitrification rates as a consequence of ocean acidification, P. Natl. Acad. Sci. USA, 108, 208–213, https://doi.org/10.1073/pnas.1011053108, 2011.

Böckmann, S., Koch, F., Meyer, B., Pausch, F., Iversen, M., Driscoll, R., Laglera, L. M., Hassler, C., and Trimborn, S.: Salp fecal pellets release more bioavailable iron to Southern Ocean phytoplankton than krill fecal pellets, Curr. Biol., 31, P2737–2746.E3, https://doi.org/10.1016/j.cub.2021.02.033, 2021.

Bopp, L., Resplandy, L., Orr, J. C., Doney, S. C., Dunne, J. P., Gehlen, M., Halloran, P., Heinze, C., Ilyina, T., Séférian, R., Tjiputra, J., and Vichi, M.: Multiple stressors of ocean ecosystems in the 21st century: projections with CMIP5 models, Biogeosciences, 10, 6225–6245, https://doi.org/10.5194/bg-10-6225-2013, 2013.

Boxhammer, T., Bach, L. T., Czerny, J., and Riebesell, U.: Technical note: Sampling and processing of mesocosm sediment trap material for quantitative biogeochemical analysis, Biogeosciences, 13, 2849–2858, https://doi.org/10.5194/bg-13-2849-2016, 2016.

Boyd, P. W., Sherry, N. D., Berges, J. A., Bishop, J. K. B., Calvert, S. E., Charette, M. A., Giovannoni, S. J., Goldblatt, R., Harrison, P. J., Moran, S. B., Roy, S., Soon, M., Strom, S., Thibault, D., Vergin, K. L., Whitney, F. A., and Wong, C.

S.: Transformations of biogenic particulates from the pelagic to the deep ocean realm, Deep-Sea Res. Pt. II, 46, 2761–2792, https://doi.org/10.1016/S0967-0645(99)00083-1, 1999.

Brečević, L. and Nielsen, A. E.: Solubility of amorphous calcium carbonate, J. Cryst. Growth, 98, 504–510, https://doi.org/10.1016/0022-0248(89)90168-1, 1989.

Byrne, C. D., Law, R. J., Hudson, P. M., Thain, J. E., and Fileman, T. W.: Measurements of the dispersion of liquid industrial waste discharged into the wake of a dumping vessel, Water Res., 22, 1577–1584, https://doi.org/10.1016/0043-1354(88)90171-6, 1988.

Cabanes, D. J. E., Norman, L., Santos-Echeandía, J., Iversen, M. H., Trimborn, S., Laglera, L. M., and Hassler, C. S.: First Evaluation of the Role of Salp Fecal Pellets on Iron Biogeochemistry, Front Mar. Sci., 3, 289, https://doi.org/10.3389/fmars.2016.00289, 2017.

Cherabier, P. and Ferrière, R.: Eco-evolutionary responses of the microbial loop to surface ocean warming and consequences for primary production, ISME J., 16, 1130–1139, https://doi.org/10.1038/s41396-021-01166-8, 2022.

Ciais, P., Sabine, C., Bala, G., Bopp, L., Brovkin, V., Canadell, J., Chhabra, A., DeFries, R., Galloway, J., and Heimann, M.: Carbon and Other Biogeochemical Cycles, in: Climate Change 2013 – The Physical Science Basis: Working Group I Contribution to the Fifth Assessment Report of the Intergovernmental Panel on Climate Change, edited by: Change, I. P. on C., Cambridge University Press, Cambridge, 465–570, https://doi.org/10.1017/CBO9781107415324.015, 2014.

Coverly, S., Kérouel, R., and Aminot, A.: A re-examination of matrix effects in the segmented-flow analysis of nutrients in sea and estuarine water, Anal. Chim. Acta, 712, 94–100, https://doi.org/10.1016/j.aca.2011.11.008, 2012.

Dai, M., Luo, Y., Achterberg, E. P., Browning, T. J., Cai, Y., Cao, Z., Chai, F., Chen, B., Church, M. J., Ci, D., Du, C., Gao, K., Guo, X., Hu, Z., Kao, S., Laws, E. A., Lee, Z., Lin, H., Liu, Q., Liu, X., Luo, W., Meng, F., Shang, S., Shi, D., Saito, H., Song, L., Wan, X. S., Wang, Y., Wang, W., Wen, Z., Xiu, P., Zhang, J., Zhang, R., and Zhou, K.: Upper Ocean Biogeochemistry of the Oligotrophic North Pacific Subtropical Gyre: From Nutrient Sources to Carbon Export, Rev. Geophys., 61, e2022RG000800, https://doi.org/10.1029/2022RG000800, 2023.

Dickson, A.: Standards for Ocean Measurements, Oceanography, 23, 34–47, https://doi.org/10.5670/oceanog.2010.22, 2010.

Doney, S. C., Fabry, V. J., Feely, R. A., and Kleypas, J. A.: Ocean Acidification, Annu. Rev. Mar. Sci., 1, 169–192, https://doi.org/10.1146/annurev.marine.010908.163834, 2009.

Endres, S., Galgani, L., Riebesell, U., Schulz, K.-G., and Engel, A.: Stimulated Bacterial Growth under Elevated pCO$_2$: Results from an Off-Shore Mesocosm Study, PLoS One, 9, e99228, https://doi.org/10.1371/journal.pone.0099228, 2014.

Engel, A., Abramson, L., Szlosek, J., Liu, Z., Stewart, G., Hirschberg, D., and Lee, C.: Investigating the effect of ballasting by CaCO$_3$ in Emiliania huxleyi, II, Deep-Sea Res. Pt. II, 56, 1408–1419, https://doi.org/10.1016/j.dsr2.2008.11.028, 2009.

Feng, E. Y., Koeve, W., Keller, D. P., and Oschlies, A.: Model-Based Assessment of the CO$_2$ Sequestration Potential of Coastal Ocean Alkalinization, Earth's Future, 5, 1252–1266, https://doi.org/10.1002/2017EF000659, 2017.

Ferderer, A., Chase, Z., Kennedy, F., Schulz, K. G., and Bach, L. T.: Assessing the influence of ocean alkalinity enhancement on a coastal phytoplankton community, Biogeosciences, 19, 5375–5399, https://doi.org/10.5194/bg-19-5375-2022, 2022.

Francois, R., Honjo, S., Krishfield, R., and Manganini, S.: Factors controlling the flux of organic carbon to the bathypelagic zone of the ocean, Global Biogeochem. Cy., 16, 34-1–34-20, https://doi.org/10.1029/2001GB001722, 2002.

Freudenthal, T., Neuer, S., Meggers, H., Davenport, R., and Wefer, G.: Influence of lateral particle advection and organic matter degradation on sediment accumulation and stable nitrogen isotope ratios along a productivity gradient in the Canary Islands region, Mar. Geol., 177, 93–109, https://doi.org/10.1016/S0025-3227(01)00126-8, 2001.

Fumasoli, A., Bürgmann, H., Weissbrodt, D. G., Wells, G. F., Beck, K., Mohn, J., Morgenroth, E., and Udert, K. M.: Growth of Nitrosococcus-Related Ammonia Oxidizing Bacteria Coincides with Extremely Low pH Values in Wastewater with High Ammonia Content, Environ. Sci. Technol., 51, 6857–6866, https://doi.org/10.1021/acs.est.7b00392, 2017.

Gately, J. A., Kim, S. M., Jin, B., Brzezinski, M. A., and Iglesias-Rodriguez, M. D.: Coccolithophores and diatoms resilient to ocean alkalinity enhancement: A glimpse of hope?, Sci. Adv., 9, eadg6066, https://doi.org/10.1126/sciadv.adg6066, 2023.

Gattuso, J.-P., Magnan, A., Billé, R., Cheung, W. W. L., Howes, E. L., Joos, F., Allemand, D., Bopp, L., Cooley, S. R., Eakin, C. M., Hoegh-Guldberg, O., Kelly, R. P., Pörtner, H.-O., Rogers, A. D., Baxter, J. M., Laffoley, D., Osborn, D., Rankovic, A., Rochette, J., Sumaila, U. R., Treyer, S., and Turley, C.: Contrasting futures for ocean and society from different anthropogenic CO$_2$ emissions scenarios, Science, 349, aac4722, https://doi.org/10.1126/science.aac4722, 2015.

GESAMP: High level review of a wide range of proposed marine geoengineering techniques, 98th ed., edited by: GESAMP, International Maritime Organization, London, https://doi.org/10.25607/OBP-1944, 2019.

González, M. F. and Ilyina, T.: Impacts of artificial ocean alkalinization on the carbon cycle and climate in Earth system simulations, Geophys. Res. Lett., 43, 6493–6502, https://doi.org/10.1002/2016GL068576, 2016.

Griffioen, J.: Enhanced weathering of olivine in seawater: the efficiency as revealed by thermodynamic scenario analysis, Sci. Total Environ., 575, 536–544, https://doi.org/10.1016/j.scitotenv.2016.09.008, 2017.

Guidi, L., Legendre, L., Reygondeau, G., Uitz, J., Stemmann, L., and Henson, S. A.: A new look at ocean carbon remineralization for estimating deepwater sequestration, Global Biogeochem. Cy., 29, 1044–1059, https://doi.org/10.1002/2014GB005063, 2015.

Hansen, H. P. and Koroleff, F.: Determination of nutrients, in: Methods of Seawater Analysis, 159–228, https://doi.org/10.1002/9783527613984.ch10, 1999.

Hartmann, J., West, A. J., Renforth, P., Köhler, P., La Rocha, C. L., Wolf-Gladrow, D. A., Dürr, H. H., and Scheffran, J.: Enhanced chemical weathering as a geoengineering strategy to reduce atmospheric carbon dioxide, supply nutrients, and mitigate ocean acidification, Rev. Geophys., 51, 113–149, https://doi.org/10.1002/rog.20004, 2013.

Hartmann, J., Suitner, N., Lim, C., Schneider, J., Marín-Samper, L., Arístegui, J., Renforth, P., Taucher, J., and Riebesell, U.: Stability

of alkalinity in ocean alkalinity enhancement (OAE) approaches – consequences for durability of CO_2 storage, Biogeosciences, 20, 781–802, https://doi.org/10.5194/bg-20-781-2023, 2023.

Hessen, D. O., Ågren, G. I., Anderson, T. R., Elser, J. J., and De Ruiter, P. C.: Carbon sequestration in ecosystems: the role of stoichiometry, Ecology, 85, 1179–1192, https://doi.org/10.1890/02-0251, 2004.

Honjo, S., Manganini, S. J., Krishfield, R. A., and Francois, R.: Particulate organic carbon fluxes to the ocean interior and factors controlling the biological pump, Prog. Oceanogr., 76, 217–285, https://doi.org/10.1016/j.pocean.2007.11.003, 2008.

Iversen, M. H.: Carbon Export in the Ocean: A Biologist's Perspective, Ann. Rev. Mar. Sci., 15, 357–381, https://doi.org/10.1146/annurev-marine-032122-035153, 2023.

Iversen, M. H. and Ploug, H.: Temperature effects on carbon-specific respiration rate and sinking velocity of diatom aggregates – potential implications for deep ocean export processes, Biogeosciences, 10, 4073–4085, https://doi.org/10.5194/bg-10-4073-2013, 2013.

Jokiel, P. L.: The reef coral two compartment proton flux model, J Exp Mar. Biol. Ecol, 409, 1–12, https://doi.org/10.1016/j.jembe.2011.10.008, 2011.

Jordan, R. W.: Coccolithophores, in: Encyclopedia of Microbiology (Third Edition), edited by: Schaechter, M., Academic Press, Oxford, 593–605, https://doi.org/10.1016/B978-012373944-5.00249-2, 2009.

Karthäuser, C., Ahmerkamp, S., Marchant, H. K., Bristow, L. A., Hauss, H., Iversen, M. H., Kiko, R., Maerz, J., Lavik, G., and Kuypers, M. M. M.: Small sinking particles control anammox rates in the Peruvian oxygen minimum zone, Nat. Commun., 12, 3235, https://doi.org/10.1038/s41467-021-23340-4, 2021.

Kheshgi, H. S.: Sequestering atmospheric carbon dioxide by increasing ocean alkalinity, Energy, 20, 915–922, https://doi.org/10.1016/0360-5442(95)00035-F, 1995.

Klaas, C. and Archer, D. E.: Association of sinking organic matter with various types of mineral ballast in the deep sea, Global Biogeochem. Cy., 16, 63-1–63-14, https://doi.org/10.1029/2001GB001765, 2002.

Koeve, W.: Upper ocean carbon fluxes in the Atlantic Ocean, Global Biogeochem. Cy., 16, 4-1–4-17, https://doi.org/10.1029/2001GB001836, 2002.

Köhler, P., Hartmann, J., and Wolf-Gladrow, D. A.: Geoengineering potential of artificially enhanced silicate weathering of olivine, P. Natl. Acad. Sci. USA, 107, 20228–20233, https://doi.org/10.1073/pnas.1000545107, 2010.

Kwon, E. Y., Primeau, F., and Sarmiento, J. L.: The impact of remineralization depth on the air–sea carbon balance, Nat. Geosci., 2, 630–635, https://doi.org/10.1038/ngeo612, 2009.

Le Moigne, F. A. C., Henson, S. A., Cavan, E., Georges, C., Pabortsava, K., Achterberg, E. P., Ceballos-Romero, E., Zubkov, M., and Sanders, R. J.: What causes the inverse relationship between primary production and export efficiency in the Southern Ocean?, Geophys. Res. Lett., 43, 4457–4466, https://doi.org/10.1002/2016GL068480, 2016.

Li, C., Luo, X., Huang, X., and Gu, B.: Effects of Temperature, Salinity, pH, and Light on Filtering and Grazing Rates of a Calanoid Copepod (Schmackeria dubia), Sci. World J., 8, 838071, https://doi.org/10.1100/tsw.2008.153, 2008.

Lüdecke, D., Ben-Shachar, M., Patil, I., Waggoner, P., and Makowski, D.: performance, J. Open Source Softw., 6, 3139, https://doi.org/10.21105/joss.03139, 2021.

Lueker, T. J., Dickson, A. G., and Keeling, C. D.: Ocean pCO_2 calculated from dissolved inorganic carbon, alkalinity, and equations for K_1 and K_2, Mar. Chem., 70, 105–119, https://doi.org/10.1016/S0304-4203(00)00022-0, 2000.

Marion, G. M., Millero, F. J., and Feistel, R.: Precipitation of solid phase calcium carbonates and their effect on application of seawater S_A-T-P models, Ocean Sci., 5, 285–291, https://doi.org/10.5194/os-5-285-2009, 2009.

Martínez-García, A., Sigman, D. M., Ren, H., Anderson, R. F., Straub, M., Hodell, D. A., Jaccard, S. L., Eglinton, T. I., and Haug, G. H.: Iron fertilization of the Subantarctic Ocean during the last ice age, Science, 343, 1347–1350, https://doi.org/10.1126/science.1246848, 2014.

Masson-Delmotte, V., Zhai, P., Pörtner, H.-O., Roberts, D., Skea, J., Shukla, P. R., al., et, and IPCC (Eds.): Climate Change 2021: The Physical Science Basis, Cambridge University Press, 2021.

McCave, I. N.: Particulate size spectra, behavior, and origin of nepheloid layers over the Nova Scotian Continental Rise, J. Geophys. Res.-Oceans, 88, 7647–7666, https://doi.org/10.1029/JC088iC12p07647, 1983.

Monteiro, F., Bach, L. T., Brownlee, C., Bown, P., E, R. R., Poulton, A. J., Tyrrell, T., Beaufort, L., Dutkiewicz, S., Gibbs, S., Gutowska, M. A., Lee, R., Riebesell, U., Young, J., and Ridgwell, A.: Why marine phytoplankton calcify, Sci. Adv., 2, e1501822, https://doi.org/10.1126/sciadv.1501822, 2016.

Moras, C. A., Bach, L. T., Cyronak, T., Joannes-Boyau, R., and Schulz, K. G.: Ocean alkalinity enhancement – avoiding runaway $CaCO_3$ precipitation during quick and hydrated lime dissolution, Biogeosciences, 19, 3537–3557, https://doi.org/10.5194/bg-19-3537-2022, 2022.

Morris, A. W. and Riley, J. P.: The determination of nitrate in sea water, Anal. Chim. Acta, 29, 272–279, https://doi.org/10.1016/S0003-2670(00)88614-6, 1963.

Morse, J. W. and He, S.: Influences of T, S and P_{CO_2} on the pseudo-homogeneous precipitation of $CaCO_3$ from seawater, Mar. Chem., 41, 291–297, https://doi.org/10.1016/0304-4203(93)90261-L, 1993.

Mucci, A.: The solubility of calcite and aragonite in seawater at various salinities, temperatures, and one atmosphere total pressure, Am. J. Sci., 283, 780–799, 1983.

Mullin, J. B. and Riley, J. P.: The colorimetric determination of silicate with special reference to sea and natural waters, Anal. Chim. Acta, 12, 162–176, https://doi.org/10.1016/S0003-2670(00)87825-3, 1955.

Murphy, J. and Riley, J. P.: A modified single solution method for the determination of phosphate in natural waters, Anal. Chim. Acta, 27, 31–36, https://doi.org/10.1016/S0003-2670(00)88444-5, 1962.

National Acadmies of Sciences: A Research Strategy for Ocean-based Carbon Dioxide Removal and Sequestration, National Academies Press, Washington, D.C., https://doi.org/10.17226/26278, 2021.

Ortiz, J., Arístegui, J., Taucher, J., and Riebesell, U.: Artificial Upwelling in Singular and Recurring Mode: Consequences for Net Community Production and Metabolic

Balance, Frontiers in Marine Science, 8, 743105, https://doi.org/10.3389/fmars.2021.743105, 2022.

Paquay, F. S. and Zeebe, R. E.: Assessing possible consequences of ocean liming on ocean pH, atmospheric CO_2 concentration and associated costs, Int. J. Greenh. Gas Con., 17, 183–188, https://doi.org/10.1016/j.ijggc.2013.05.005, 2013.

Passow, U. and Carlson, C. A.: The biological pump in a high CO_2 world, Mar. Ecol. Prog. Ser., 470, 249–271, https://doi.org/10.3354/meps09985, 2012.

Paul, A. J., Haunost, M., Goldenberg, S. U., Hartmann, J., Sánchez, N., Schneider, J., Suitner, N., and Riebesell, U.: Ocean alkalinity enhancement in an open ocean ecosystem: Biogeochemical responses and carbon storage durability, EGUsphere [preprint], https://doi.org/10.5194/egusphere-2024-417, 2024.

Pierrot, D. E., Wallace, D. W. R., and Lewis, E.: MS Excel Program Developed for CO_2 System Calculations, GitHub [code], https://github.com/dpierrot/co2sys_xl (last access: 14 October 2023), 2011.

Pinheiro, J., Bates, D., and R Core Team: nlme: Linear and Nonlinear Mixed Effects Models, R package version 3.1-160, https://CRAN.R-project.org/package=nlme (last access: 14 October 2023), 2022.

Piontek, J., Lunau, M., Händel, N., Borchard, C., Wurst, M., and Engel, A.: Acidification increases microbial polysaccharide degradation in the ocean, Biogeosciences, 7, 1615–1624, https://doi.org/10.5194/bg-7-1615-2010, 2010.

Ploug, H. and Grossart, H.-P.: Bacterial growth and grazing on diatom aggregates, Limnol. Oceanogr., 45, 1467–1475, https://doi.org/10.4319/lo.2000.45.7.1467, 2000.

Pommerening-Röser, A. and Koops, H. P.: Environmental pH as an important factor for the distribution of urease positive ammonia-oxidizing bacteria, Microbiol. Res., 160, 27–35, https://doi.org/10.1016/j.micres.2004.09.006, 2005.

Puig, P., Madron, X. D. de, Salat, J., Schroeder, K., Martín, J., Karageorgis, A. P., Palanques, A., Roullier, F., Lopez-Jurado, J. L., Emelianov, M., Moutin, T., and Houpert, L.: Thick bottom nepheloid layers in the western Mediterranean generated by deep dense shelf water cascading, Prog. Oceanogr., 111, 1–23, https://doi.org/10.1016/j.pocean.2012.10.003, 2013.

R Core Team: R: A language and environment for statistical computing. R Foundation for Statistical Computing, Vienna, Austria, https://www.R-project.org/ (last access: 14 October 2023), 2021.

Renforth, P. and Henderson, G.: Assessing ocean alkalinity for carbon sequestration, Rev. Geophys., 55, 636–674, https://doi.org/10.1002/2016RG000533, 2017.

Riebesell, U., Wolf-Gladrow, D. A., and Smetacek, V.: Carbon dioxide limitation of marine phytoplankton growth rates, Nature, 361, 249–251, https://doi.org/10.1038/361249a0, 1993.

Riebesell, U., Czerny, J., von Bröckel, K., Boxhammer, T., Büdenbender, J., Deckelnick, M., Fischer, M., Hoffmann, D., Krug, S. A., Lentz, U., Ludwig, A., Muche, R., and Schulz, K. G.: Technical Note: A mobile sea-going mesocosm system – new opportunities for ocean change research, Biogeosciences, 10, 1835–1847, https://doi.org/10.5194/bg-10-1835-2013, 2013.

Riebesell, U., Bach, L. T., Bellerby, R. G. J., Monsalve, J., Boxhammer, T., Czerny, J., Larsen, A., Ludwig, A., and Schulz, K. G.: Competitive fitness of a predominant pelagic calcifier impaired by ocean acidification, Nat. Geosci., 10, 19–23, https://doi.org/10.1038/ngeo2854, 2017.

Ristow, G. H.: Wall correction factor for sinking cylinders in fluids, Phys. Rev. E, 55, 2808–2813, https://doi.org/10.1103/PhysRevE.55.2808, 1997.

Rothwell, R. G.: Sedimentary Rocks, in: Reference Module in Earth Systems and Environmental Sciences, Elsevier, https://doi.org/10.1016/B978-0-12-409548-9.10493-2, 2016.

Salter, I., Schiebel, R., Ziveri, P., Movellan, A., Lampitt, R., and Wolff, G. A.: Carbonate counter pump stimulated by natural iron fertilization in the Polar Frontal Zone, Nat. Geosci., 7, 885–889, https://doi.org/10.1038/ngeo2285, 2014.

Sarthou, G., Vincent, D., Christaki, U., Obernosterer, I., Timmermans, K. R., and Brussaard, C. P. D.: The fate of biogenic iron during a phytoplankton bloom induced by natural fertilisation: Impact of copepod grazing, Deep-Sea Res. Pt. II, 55, 734–751, https://doi.org/10.1016/j.dsr2.2007.12.033, 2008.

Schmittner, A., Oschlies, A., Schulz, K. G., and Riebesell, U.: Simulated 21st century's increase in oceanic suboxia by CO_2-enhanced biotic carbon export, Global Biogeochem. Cy., 22, GB4008, https://doi.org/10.1029/2007GB003147, 2008.

Schneider, B., Schlitzer, R., Fischer, G., and Nöthig, E.-M.: Depth-dependent elemental compositions of particulate organic matter (POM) in the ocean, Global Biogeochem. Cy., 17, 1032, https://doi.org/10.1029/2002GB001871, 2003.

Shaffer, G.: Biogeochemical cycling in the global ocean, J. Geophys. Res.-Oceans, 101, 3723–3745, https://doi.org/10.1029/95JC03373, 1996.

Sharp, J. H.: Improved analysis for "particulate" organic carbon and nitrogen from seawater, Limnol. Oceanogr., 19, 984–989, https://doi.org/10.4319/lo.1974.19.6.0984, 1974.

Smith, P., Davis, S. J., Creutzig, F., Fuss, S., Minx, J., Gabrielle, B., Kato, E., Jackson, R. B., Cowie, A., and Kriegler, E.: Biophysical and economic limits to negative CO_2 emissions, Nat. Clim. Change, 6, 42–50, https://doi.org/10.1038/nclimate2870, 2016.

Sprengel, C., Baumann, K. H., Henderiks, J., Henrich, R., and Neuer, S.: Modern coccolithophore and carbonate sedimentation along a productivity gradient in the Canary Islands region: seasonal export production and surface accumulation rates, Deep-Sea Res. Pt. II, 49, 3577–3598, https://doi.org/10.1016/S0967-0645(02)00099-1, 2002.

Stange, P., Taucher, J., Bach, L. T., Algueró-Muñiz, M., Horn, H. G., Krebs, L., Boxhammer, T., Nauendorf, A. K., and Riebesell, U.: Ocean Acidification-Induced Restructuring of the Plankton Food Web Can Influence the Degradation of Sinking Particles, Front. Mar. Sci., 5, 140, https://doi.org/10.3389/fmars.2018.00140, 2018.

Strickland, J. D. H. and Parsons, T. R.: A Practical Handbook of Seawater Analysis, 2nd edn., Ottawa, Canada, Fisheries Research Board of Canada, 310 pp., Bulletin Fisheries Research Board of Canada, 167, https://doi.org/10.25607/OBP-1791, 1972.

Stukel, M. R., Landry, M. R., Benitez-Nelson, C. R., and Goericke, R.: Trophic cycling and carbon export relationships in the California Current Ecosystem, Limnol. Oceanogr., 56, 1866–1878, https://doi.org/10.4319/lo.2011.56.5.1866, 2011.

Subhas, A. V, Marx, L., Reynolds, S., Flohr, A., Mawji, E. W., Brown, P. J., and Cael, B. B.: Microbial ecosystem responses to alkalinity enhancement in the North Atlantic Subtropical Gyre, Frontiers in Climate, 4, 784997, https://doi.org/10.3389/fclim.2022.784997, 2022.

Suessle, P., Taucher, J., Goldenberg, S. U., Baumann, M., Noche-Ferreira, A., and Vanharanta, M.: KOSMOS 2021 Gran Canaria mesocosm study on ocean alkalinity enhancement: sediment trap particle flux data and water column biogeochemistry, PANGAEA [data set], https://doi.org/10.1594/PANGAEA.967359, 2024.

Suzuki, S., Kawachi, M., Tsukakoshi, C., Nakamura, A., Hagino, K., Inouye, I., and Ishida, K.: Unstable Relationship Between *Braarudosphaera bigelowii* (= *Chrysochromulina parkeae*) and Its Nitrogen-Fixing Endosymbiont, Front. Plant. Sci., 12, 74989, https://doi.org/10.3389/fpls.2021.749895, 2021.

Taucher, J. and Oschlies, A.: Can we predict the direction of marine primary production change under global warming?, Geophys. Res. Lett., 38, LO2603, https://doi.org/10.1029/2010GL045934, 2011.

Taucher, J., Bach, L. T., Boxhammer, T., Nauendorf, A., Consortium, T. G. C. K., Achterberg, E. P., Algueró-Muñiz, M., Arístegui, J., Czerny, J., Esposito, M., Guan, W., Haunost, M., Horn, H. G., Ludwig, A., Meyer, J., Spisla, C., Sswat, M., Stange, P., and Riebesell, U.: Influence of Ocean Acidification and Deep Water Upwelling on Oligotrophic Plankton Communities in the Subtropical North Atlantic, Front. Mar. Sci., 4, 85, https://doi.org/10.3389/fmars.2017.00085, 2017.

Taucher, J., Boxhammer, T., Bach, L. T., Paul, A. J., Schartau, M., Stange, P., and Riebesell, U.: Changing carbon-to-nitrogen ratios of organic-matter export under ocean acidification, Nat. Clim. Change, 11, 52–57, https://doi.org/10.1038/s41558-020-00915-5, 2021.

Taylor, L. L., Quirk, J., Thorley, R. M. S., Kharecha, P. A., Hansen, J., Ridgwell, A., Lomas, M. R., Banwart, S. A., and Beerling, D. J.: Enhanced weathering strategies for stabilizing climate and averting ocean acidification, Nat. Clim. Change, 6, 402–406, https://doi.org/10.1038/nclimate2882, 2016.

Utermöhl, H.: Zur Vervollkommnung der quantitativen Phytoplankton Methodik, in: Mitteilungen der IVL, Number 9, Schweizerbart Science Publishers, Stuttgart, Germany, ISBN 9783510520091, 1958.

Webb, A. L., Malin, G., Hopkins, F. E., Ho, K. L., Riebesell, U., Schulz, K., Larsen, A., and Liss, P.: Ocean acidification affects production of DMS and DMSP measured in a mesocosm study and cultures of Emiliania huxleyi and a mesocosm study, Environ. Chem., 13, 314–329, https://doi.org/10.1071/EN14268, 2016.

Welschmeyer, N. A.: Fluorometric analysis of chlorophyll *a* in the presence of chlorophyll *b* and pheopigments, Limnol. Oceanogr., 39, 1985–1992, https://doi.org/10.4319/lo.1994.39.8.1985, 1994.

Wickham, H., Averick, M., Bryan, J., Chang, W., McGowan, L., François, R., Grolemund, G., Hayes, A., Henry, L., Hester, J., Kuhn, M., Pedersen, T., Miller, E., Bache, S., Müller, K., Ooms, J., Robinson, D., Seidel, D., Spinu, V., Takahashi, K., Vaughan, D., Wilke, C., Woo, K., and Yutani, H.: Welcome to the Tidyverse, J. Open Source Softw., 4, 1686, https://doi.org/10.21105/joss.01686, 2019.

Wurgaft, E., Wang, Z. A., Churchill, J. H., Dellapenna, T., Song, S., Du, J., Ringham, M. C., Rivlin, T., and Lazar, B.: Particle Triggered Reactions as an Important Mechanism of Alkalinity and Inorganic Carbon Removal in River Plumes, Geophys. Res. Lett., 48, e2021GL093178, https://doi.org/10.1029/2021GL093178, 2021.

Xin, X., Goldenberg, S., Taucher, J., Stuhr, A., Aristegui, J., and Riebesell, U.: Resilience of phytoplankton and microzooplankton communities under ocean alkalinity enhancement in the oligotrophic ocean, Environ. Sci. Technol., 58, 20918–20930, https://doi.org/10.1021/acs.est.4c09838, 2025.

Zagarese, H. E., Sagrario, M. de los Á. G., Wolf-Gladrow, D., Nõges, P., Nõges, T., Kangur, K., Matsuzaki, S.-I. S., Kohzu, A., Vanni, M. J., Özkundakci, D., Echaniz, S. A., Vignatti, A., Grosman, F., Sanzano, P., Van Dam, B., and Knoll, L. B.: Patterns of CO_2 concentration and inorganic carbon limitation of phytoplankton biomass in agriculturally eutrophic lakes, Water Res., 190, 116715, https://doi.org/10.1016/j.watres.2020.116715, 2021.

Zeebe, R. E. and Wolf-Gladrow, D. A.: CO_2 in seawater: Equilibrium, kinetics, isotopes, edited by: Zeebe, R. E. and Wolf-Gladrow, D. A., Elsevier, Amsterdam, New York, 346 pp., ISBN 9780444509468, 2010.